ELSEVIER

NeuroImage

www.elsevier.com/locate/ynimg
NeuroImage 26 (2005) 177–183

Coherence between fMRI time-series distinguishes two spatial working memory networks

Clayton E. Curtis,[a,*] Felice T. Sun,[b] Lee M. Miller,[c] and Mark D'Esposito[b]

[a]*Department of Psychology and Center for Neural Science, New York University, 6 Washington Place, Room 859, New York, NY 10003, USA*
[b]*Helen Wills Neuroscience Institute and Department of Psychology, University of California, 3210 Tolman Hall, Berkeley, CA 94720-1650, USA*
[c]*Center for Mind and Brain and Section of Neurobiology, Physiology, and Behavior, University of California, Davis, 202 Cousteau Place, Room 267, Davis, CA 95616, USA*

Received 25 August 2004; revised 8 January 2005; accepted 18 January 2005
Available online 7 March 2005

Widespread and distributed brain regions are thought to form networks that together support working memory. We recently demonstrated that different cortical areas maintain relatively different codes across a memory delay (Curtis et. al., *J Neurosci*, 2004; 24:3944–3952). The frontal eye fields (FEF), for example, were more active during the delay when the direction of the memory-guided saccade was known compared to when it was not known throughout the delay. Other areas showed the opposite pattern. Despite these task-dependent differences in regional activity, we could only assume but not address the functional interactions between the identified nodes of the putative network. Here, we use a bivariate technique, coherence, to formally characterize functional interactions between a seed region and other brain areas. We find that the type of representational codes that are being maintained in working memory biases frontal–parietal interactions. For example, coherence between FEF and other oculomotor areas was greater when a motor representation was an efficient strategy to bridge the delay period. However, coherence between the FEF and higher-order heteromodal areas, e.g., dorsolateral prefrontal cortex, was greater when a sensory representation must be maintained in working memory.

Keywords: Coherence; Functional connectivity; Network; Spatial working memory; fMRI; Oculomotor; Delayed response; Motor control

Introduction

Persistent activity during the delay period of a working memory task is compelling evidence that the activity reflects a memory representation (Funahashi et al., 1989; Fuster and Alexander, 1971; Gnadt and Andersen, 1988; Kubota and Niki, 1971). Many parts of the cortex and subcortex show such persistent activity and thus may form networks that support maintenance processes. Our recent work, however, has focused not on which parts of the brain are active during working memory delays, but instead on what might persistent activity represent. In other words, what is being coded for by persistent activity? During a memory delay, one may need to keep active a past perceptual event, a *retrospective* sensory code, or a future action, a *prospective* motor code, in order to link events that are separated in time but are contingent upon one another (Boussaoud and Wise, 1993; D'Esposito et al., 2000b; Funahashi et al., 1993; Quintana and Fuster, 1999; Rainer et al., 1999).

In our recent study (Curtis et al., 2004), we used event-related functional magnetic resonance imaging (fMRI) to measure brain activity while subjects performed two oculomotor delayed-response tasks: (1) a classic oculomotor delayed-response task (Fig. 1a, Match), where on each trial subjects simply made a saccade that shifted gaze to a location that matched the remembered location of a sample cue presented 10 s earlier and (2) an oculomotor delayed non-matching-to-sample task (Fig. 1a, Non-Match), where a memory-guided saccade was made to a location that did not match the location of the sample. In the Match condition, subjects could plan a saccade that would acquire the target and maintain this goal by simply delaying the initiation of the saccade until after the delay. In the Non-Match condition, our goal was to bias subjects away from maintaining a visuomotor code, but instead encourage the maintenance of a visuospatial code. Using standard univariate statistics, we found that oculomotor areas, like the FEF, were more active during Match delays compared to Non-Match delays (Fig. 1b). This suggests that the FEF contributes to spatial working memory by maintaining saccade goals.

These findings led us to propose that a network of brain areas maintains the task relevant information, where different nodes in this network maintain different representational codes, such as motor and sensory representations. Inherent in this proposition is that these nodes are interacting in some way, passing, transforming, and/or sustaining representations. However, we could only assume but not directly measure the functional interactions between the identified nodes of the putative network. Here, we re-analyze the fMRI data with a bivariate technique, coherence, to formally

* Corresponding author.
E-mail address: clayton.curtis@nyu.edu (C.E. Curtis).
Available online on ScienceDirect (www.sciencedirect.com).

1053-8119/$ - see front matter © 2005 Elsevier Inc. All rights reserved.
doi:10.1016/j.neuroimage.2005.01.040

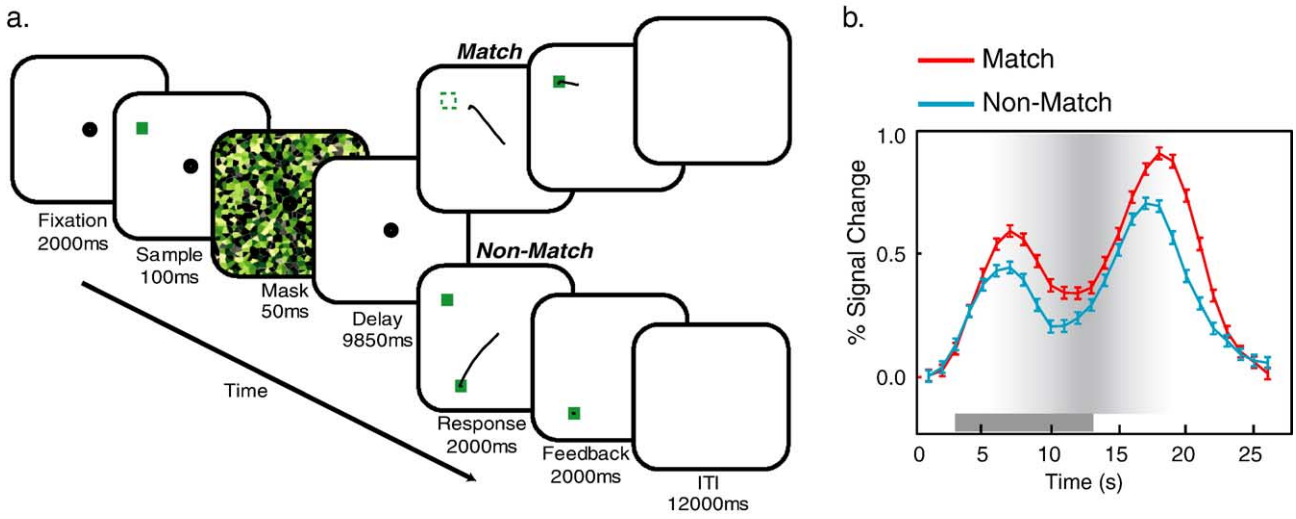

Fig. 1. (a) Schematic depiction of the oculomotor delayed-response tasks where subjects used the cue's location to make a memory-guided saccade. Both the matching-to-sample (top) and non-matching-to-sample (bottom) tasks began with the brief presentation of a small green sample cue while the subject maintained central fixation. The cue appeared randomly at 1 of 16 possible locations at a 10° radius, none of which lie on the cardinal axes. A masking pattern was then briefly presented to disrupt iconic visual memory followed by a long unfilled memory delay. During matching trials, the subject made a memory-guided saccade after the disappearance of the fixation cue marking the end of the delay. Feedback was provided by the representation of the cue. At this point, the subject corrected any errors by shifting gaze to the cue (depicted by the thin black line). During non-matching trials, the subject made a saccade to the green square that did not match the location of the sample cue. (b) Trial-averaged BOLD response data from Curtis et al. (2004) from the right FEF, the seed region used in the current study. Note that this region showed greater activity on Match than Non-Match trials that is prominent throughout the delay period.

characterize functional interactions between a seed region and other brain areas. The coherence statistic, which can be thought of as a correlation in frequency space, allows us to identify brain areas that change their functional connectivity with the FEF as a function of the matching and non-matching to-sample task demands. These data have been presented in abstract form (C.E.C. et al., Cognitive Neuroscience Society Abstracts F242, 2003).

Methods

Experimental methods

Fifteen healthy participants (8 females; ages 18–33), who gave informed consent according to procedures approved by the University of California, performed 3 runs of each of the oculomotor delayed-response tasks, matching and non-matching-to-sample, as depicted in Fig. 1. Both the matching-to-sample and non-matching-to-sample tasks began with the brief presentation of a small green sample cue for 100 ms while the subject maintained central fixation. The cue appeared randomly at 1 of 16 possible locations at a 10° radius, none of which lie on the cardinal axes. A masking pattern was then briefly presented for 50 ms to disrupt iconic visual memory followed by a long 9850 ms unfilled memory delay. During matching trials, the subject made a memory-guided saccade after the disappearance of the fixation cue that marked the end of the delay. Feedback was provided after 2000 ms by the re-presentation of the cue. At this point, the subject corrected any errors by shifting gaze to the cue. During non-matching trials, the subject made a saccade to the green square that did not match the location of the sample cue. The order of the runs was counterbalanced and yielded a total of 48 trials of each type. The matching and non-matching-to-sample tasks were performed in separate runs to encourage the use of a stationary strategy or set.

Neuroimaging methods

T2*-weighted echo planar images (EPI) sensitive to blood oxygenation level-dependent (BOLD) contrasts were acquired at 4 Tesla with a Varian INOVA MR scanner (www.varianinc.com) and a TEM send-and-receive RF head coil using a 2-shot gradient-echo EPI sequence (22.4 cm square field-of-view with a 64 × 64 matrix size resulting in an in-plane resolution of 3.5 × 3.5 mm for each of 18 3.5 mm axial slices with no interslice gap; repetition time = 1 s per half of k-space (2 s total), echo time = 28 ms, flip angle = 20°). Functional volumes were acquired during six runs lasting 448 s each, resulting in 2688 volumes total, covering the dorsal cortex. High-resolution MP-Flash 3D T1-weighted scans were acquired for anatomical localization.

Preprocessing

Functional images acquired from the scanner were reconstructed from k-space using a linear time-interpolation algorithm to double the effective sampling rate. Image volumes were corrected for slice-timing skew using temporal sinc-interpolation and corrected for movement using rigid-body transformation parameters.

Oculomotor methods

Eye position was monitored in the scanner at 60 Hz with an infrared videographic camera equipped with a telephoto lens (Model 504LRO, Applied Sciences Laboratories, www.a-s-l.com) that was focused on the right eye via a small dielectric flat surface mirror mounted inside the RF coil. Nine-point calibrations were performed at the beginning of the session and between runs when necessary. Eye movement data were calibrated and transformed to degrees of visual angle using a 3rd order polynomial algorithm that fit eye positions to known

spatial positions and then scored offline with in-house software (GRAPES). The difference between the endpoint fixation after the memory-guided saccade and the fixation to acquire the feedback cue was used as an index of memory accuracy. Saccadic reaction times were estimated with semi-automatic routines that relied on the eye's acceleration to determine the onset of saccades. Eye position data were not available for 2 subjects due to technical difficulties.

Coherence analysis

To investigate inter-regional interactions, we performed a seed-coherence analysis, calculating the coherence between a seed region and all other brain voxels. Coherence measures how well one signal can be represented by a linear transformation of another. It is thus an indication of the functional connectivity between brain areas (Muller et al., 2001, 2003; Sun et al., 2004). In the context of neuroimaging, functional connectivity should be understood as temporal covariation of a neurophysiological index such as BOLD. It may be distinguished from effective connectivity, more commonly applied in animal neurophysiology (Gerstein and Perkel, 1969; Miller et al., 2001), which requires stronger evidential support for causation, directionality, and/or timing of neural network influences (Friston et al., 1993).

Definition of coherence

The coherence between time-series x and y is defined by

$$\mathrm{Coh}_{xy}(\lambda) = \frac{|f_{xy}(\lambda)|^2}{\left[f_{xx}(\lambda) f_{yy}(\lambda)\right]}$$

where $f_{xy}(\lambda)$ is the cross-spectrum of x and y, and $f_{xx}(\lambda)$ is the power spectrum of x (Brillinger, 2001; Muller et al., 2001). It is a normalized measure from 0 to 1, where 0 indicates an absence of any linear relation, and 1 indicates that the signals are perfectly related by a linear magnitude and phase transform. When comparing the coherence between conditions, we transformed the coherence value with an arc-hyperbolic tangent function to approximate a normal distribution.

Note that an estimate of an HRF is not needed to calculate coherence statistics. In essence, the time-series of seed voxels are compared with the time-series of all other voxels in the brain. The coherence statistic is the spectral analog of cross-correlation. Unlike coherence, cross-correlation is sensitive to phase lags and differences in the hemodynamic response function across regions. This is a critical difference because we know that the shape of the HRF varies across the brain (Handwerker et al., 2004; Miezin et al., 2000). Unfortunately with fMRI data, the coherence between two time-series cannot be isolated to a specific task period, like to the retention interval of a delayed-response task. However, it is not the case that significant coherence is only limited to voxels that show a task-locked effect that would be detected with traditional univariate statistical analyses. One cannot conclude that the functional connectivity is being driven by monosynaptic connections between areas with high coherence. Nonetheless, coherence is a measure of "functional connectivity," the temporal correlation of physiological processes between spatially discrete brain areas (Friston et al., 1993), and shows great promise in functional imaging network analyses (Sun et al., 2004).

The coherence analysis we used is summarized by the following steps and described in further detail below:

1.) Identify seed voxels within an anatomically defined mask.
2.) Generate condition-specific coherence maps for the seed voxels.
3.) Compare coherence between conditions.

Identifying seed voxels

We selected seed regions of interest (ROIs) in the right FEF of each subject based on the activated regions in Curtis et al. (2004). These voxels in the FEF were identified as the voxels with the most task-related activity by choosing the maximum significant F-value for all Match and Non-Match periods based on a multiple regression analysis using the Fourier set as basis functions for each trial period. Statistical analyses were implemented in Voxbo (www.voxbo.org). A single, averaged time-series was derived from each seed region.

Generating time-series and coherence maps

Time-series for every brain voxel were separated into non-overlapping, condition-specific segments (i.e. matching and non-matching), mean-centered, and tapered with a 4-point split-cosine bell function to minimize spectral leakage due to segmented edge effects. These segments were then concatenated to form continuous condition-specific time-series. Essentially, four time-series of equal length were generated for each subject: (1) a single vector of signal intensities averaged over seed ROI voxels for all Match trials concatenated; (2) a single vector of signal intensities averaged over seed ROI voxels for all Non-Match trials concatenated; (3) vectors of signal intensities for each brain voxel for Match trials concatenated; (4) vectors of signal intensities for each brain voxel for Non-Match trials concatenated. We estimated the band-averaged (0–0.15 Hz) condition-specific coherence of the seed region's time-series with all other voxels' time-series using Welch's averaged periodogram method in Matlab (www.mathworks.com). The frequency band chosen contains the frequencies of an evoked hemodynamic response and has been shown to provide better estimates of interregional coherence than higher frequencies (Sun et al., 2004). Condition-specific coherence maps were generated for each seed region using this coherence measure.

Comparing coherence between conditions

To contrast functional interactions with the seed region across conditions, we atanh-transformed and subtracted the Match coherence map from the Non-Match coherence map for each subject. A random-effects test was performed across subjects on these difference maps, with significance set at $P < 0.005$, uncorrected, after the individual subject data were spatially normalized into standard atlas space (Montreal Neurological Institute reference brain) using routines from SPM99 (www.fil.ion.ucl.ac.uk/spm), resampled to 2 mm isotropic voxels, and spatially smoothed with an 8 mm FWHM Gaussian kernel.

Results

Oculomotor results

As reported in Curtis et al. (2004), the average positional error of memory-guided saccades on the matching-to-sample task was 2.13

(±0.43)°. On the non-matching-to-sample task, erroneous saccades to the matching cue were rare (3.37% of trials [range 0–8.33%]) and were almost always corrected before the feedback was given. Importantly, the mean saccadic reaction times between the matching (mean = 315.2 ms; standard deviation = 59.2 ms) and non-matching (mean = 365.0 ms; standard deviation = 67.5 ms) tasks differed significantly ($t(9) = 2.34$; $P < 0.05$). The faster saccadic reaction times for Match trials is consistent with the hypothesis that subjects prepared the memory-guided saccade during the delay.

Coherence between fMRI time-series results

Fig. 2a shows the coherence map of the right FEF seed in a single representative subject for the Match condition. Higher coherence values mean that there is a linear relationship between the seed region and the highlighted voxel. Note that a large network of frontal, premotor, supplementary motor, parietal, and occipital foci are coherent with the right FEF seed. Fig. 2b shows the coherence map of the right FEF in the same subject, but for the Non-Match condition. Several areas overlap between the two coherence maps, but some areas appear to show distinct coherence with the right FEF seed. It is important to note that several distant areas show coherence that are as strong as the voxels that surround the right FEF seed indicating that these maps are yielding information beyond the point-spread function of the hemodynamic response and the extrinsic spatial smoothing.

Match > Non-Match

To quantify how functional interactions change with the task, for each subject, we subtracted the right FEF coherence maps for Match and Non-Match. To estimate the reliability of these contrasts, a *t* test was performed on the coherence difference maps (Table 1). As depicted in Fig. 2c, several areas showed increased coherence on the Match compared to the Non-Matching condition (warm colors). The supplementary eye fields (SEF), the dorsal anterior cingulate cortex (dACC), the left FEF, and several foci

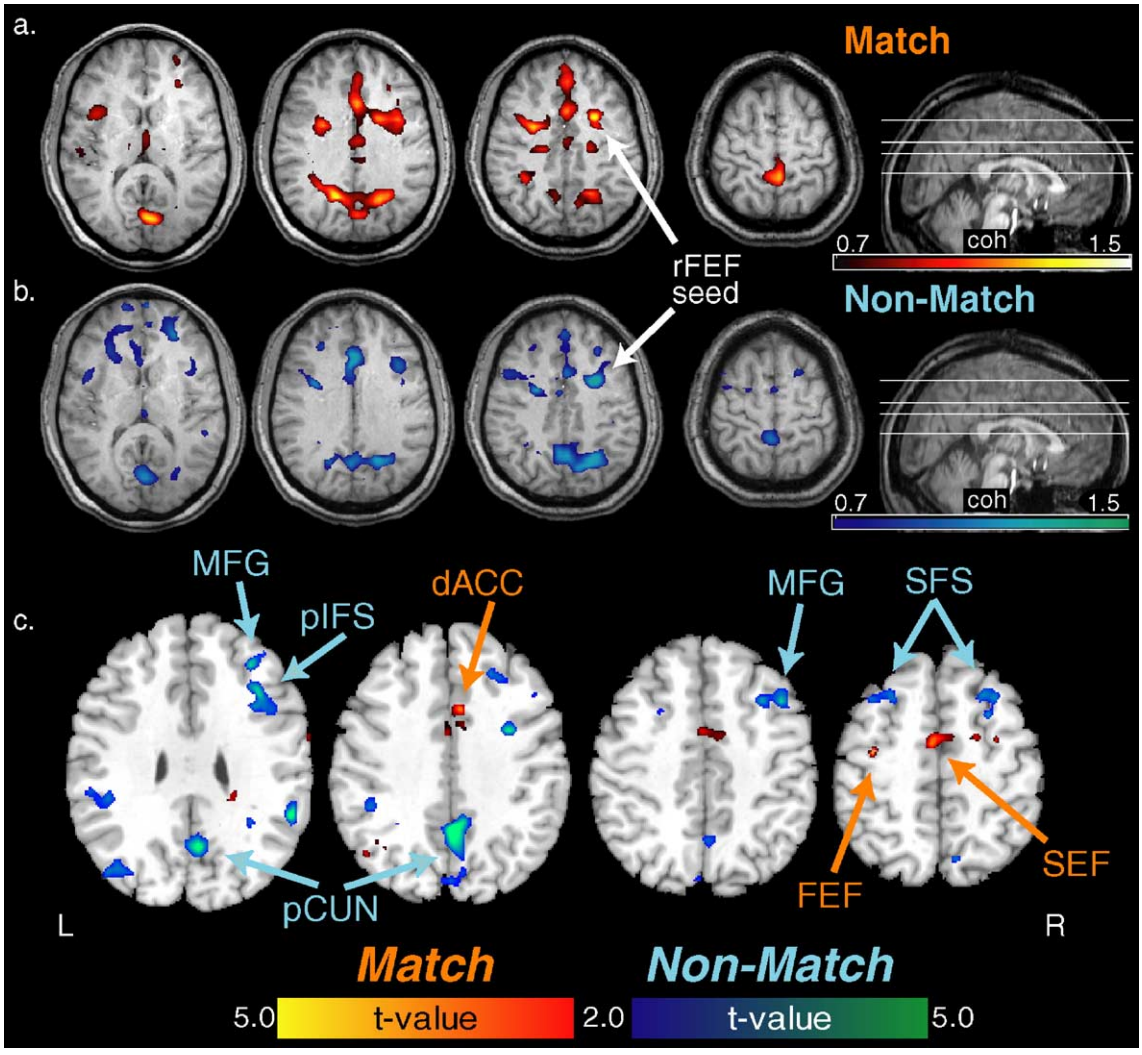

Fig. 2. Statistical coherence maps. Representative subject's coherence map for (a) Match trials and (b) Non-Match trials overlaid on the subject's anatomy. (c) Statistical parametric map (*t* statistic) showing the reliability of right FEF coherence difference maps overlaid on an MNI atlas brain. These were created by subtracting the Match and Non-Match coherence maps for each subject. Warm colors indicate regions that show greater coherence with the right FEF seed on Match compared to Non-Match trials. Cool colors indicate regions that show greater coherence with the right FEF seed on Non-Match compared to Match trials. pIFS = posterior inferior frontal sulcus; dACC = dorsal anterior cingulated cortex; SEF = supplementary eye fields; MFG = middle frontal gyrus; SFS = superior frontal sulcus; FEF = frontal eye fields; pCUN = precuneous.

Table 1
Oculomotor matching-to-sample versus non-matching-to-sample coherence differences

Region	Hemisphere	Peak MNI Coordinates			BA
		X	*Y*	*Z*	
Match > Non-Match					
FEF	Right	30	−5	64	6
SEF	Left	−5	−4	64	6
dACC	Right	4	12	42	32
Non-Match > Match					
SFS	Right	28	10	64	8
SFS	Right	31	18	55	8
SFS	Left	−32	21	62	8
MFG	Right	42	18	53	9/46
pIFS/iPCS	Right	36	14	32	44
SMG	Right	55	−50	24	40
IPL	Right	58	−50	39	40
pCUN	Right	4	−58	44	7

FEF = frontal eye fields; SEF = supplementary eye fields; dACC = dorsal anterior cingulate cortex; MFG = middle frontal gyrus; SFS = superior frontal sulcus; pIFS = posterior inferior frontal sulcus; iPCS = inferior precentral sulcus; SMG = supramarginal gyrus; IPL = inferior parietal lobule.

surrounding the right FEF seed region all show significantly greater coherence during the matching compared to non-matching task.

Non-Match > Match

Also depicted in Fig. 2c, several areas showed increased coherence on the non-matching compared to matching condition (cool colors). Several frontal cortex regions showed greater non-matching coherence, including the right middle frontal gyrus (MFG), posterior inferior frontal sulcus (pIFS), and bilateral superior frontal sulcus (SFS). Additionally, the precuneous (pCUN) region of the parietal cortex also showed greater coherence during the non-matching compared to matching task.

Discussion

Past human neuroimaging studies have generally implicated a widespread and distributed frontal–parietal network in the maintenance of spatial information (Brown et al., 2004; Courtney et al., 1998; LaBar et al., 1999; Leung et al., 2002; Postle et al., 2000; Rowe et al., 2000; Sakai et al., 2002; Sweeney et al., 1996). Much of this work has emphasized different elements of this network but has not explored the functional interactions among regions. Since traditional univariate statistics cannot address issues of functional connectivity, a multivariate technique is necessary. The ability to address issues of network interactions or functional connectivity would be a significant advance towards the often touted, but rarely realized, advantage of whole brain fMRI.

Coherence is a bivariate statistic that has been applied successfully across brain regions in electroencephalography, magnetoencephalography, and single-cell electrophysiology (Friston, 1997; Miller and Schreiner, 2000; Rosenberg et al., 1989; Shaw, 1984) and within visual cortex (Muller et al., 2001) and motor cortex (Sun et al., 2004) using fMRI. Coherence can be used as an index of functional connectivity. Specifically, it reflects the degree to which a voxel's time-series can be predicted by the time-series of the seed region. While coherence may in part reflect expected, task-induced activity common across regions, it takes advantage of trial-to-trial variability in response timing and magnitude as well as other unpredictable activity changes, which cannot be captured by univariate analyses. Importantly, differences in coherence between two conditions can be used to estimate changes in functional connectivity invoked by performance of the two tasks. Though correlation has also proved valuable (Biswal et al., 1995; Cordes et al., 2000), one distinct advantage coherence has over its time-domain counterpart, making it particularly appropriate for BOLD signals (Muller et al., 2001; Sun et al., 2004), is that it is independent of an estimate of the hemodynamic response function and therefore avoids the associated biases in analysis.

We used coherence to formally characterize functional interactions between a seed region in the right FEF and other brain areas. Coherence was estimated using time-series fMRI data from a recent fMRI study of spatial working memory in which the FEF played a special role (Curtis et al., 2004). In that study, we manipulated whether the memory-guided response could be selected before or after the delay with the use of matching and non-matching-to-sample oculomotor delayed-response tasks. We reasoned that knowing the forthcoming response throughout the retention interval, as was the case on the Match trials, would bias the subject toward maintaining a prospective motor code. The Non-Match condition was thought to bias the subject against such a strategy. Indeed, univariate analyses indicated that the FEF showed greater delay period activity during the Match compared to Non-Match condition suggesting that it contributes to spatial working memory by maintaining saccade goals.

The current study's coherence analyses further suggest that the strategy used to maintain spatial information – here we presume the strategy to be a representation of a prospective motor code (e.g., a saccade vector to acquire the cue's locations) or a retrospective visuospatial code (e.g., sustained covert attention at the cue's location) – biases the FEF's interactions with other frontal and parietal cortical areas. On Match trials, when the direction of the upcoming memory-guided saccade was known, oculomotor areas showed a stronger coherence with the FEF seed than on Non-Match trials, when the saccade was not known.

The SEF and dACC, both of which are medial premotor areas known to influence oculomotor behavior, have bi-directional connections with the FEF (Bates and Goldman-Rakic, 1993; Huerta and Kaas, 1990; Huerta et al., 1987; Lu et al., 1994; Luppino et al., 1993; Stanton et al., 1995). When a prospective motor code is the optimal means by which a location can be remembered, then functional interactions between oculomotor areas, namely between the FEF and the SEF/dACC, may form a primary network that supports spatial working memory. However, when this strategy is not optimal, in the case of Non-Match trials where the direction of the memory-guided saccade is unknown throughout the delay, another strategy may be employed. The difference in maintenance strategies may directly influence the functional interactions between brain areas. Indeed, a different pattern of FEF functional connectivity was found on Non-Match compared to Match trials. The FEF seed showed greater Non-Match coherence with several frontal areas that are thought to play a higher-level role in cognition than the premotor areas that showed greater Match coherence. These included the right MFG and right pIFS, areas that have repeatedly been linked to spatial working

memory performance (Brown et al., 2004; Courtney et al., 1998; Curtis and D'Esposito, 2003; D'Esposito et al., 2000a; Grosbras et al., 2001; LaBar et al., 1999; Leung et al., 2002; Postle et al., 2000; Rowe et al., 2000; Sakai et al., 2002; Sereno et al., 2001; Simon et al., 2002; Smith and Jonides, 1999; Sweeney et al., 1996; Zarahn et al., 1999). Furthermore, the FEF showed greater Non-Match coherence with bilateral portions of the SFS, a region that Courtney et al. (1998) reported to have a particularly specific response to the maintenance of spatial compared to face stimuli.

Treating individual brain regions as independent components, as we did in our previous study (Curtis et al., 2004), we demonstrated that the strategic demands of the working memory task biased the activity of several brain regions including the FEF. We concluded with a broad speculation that the strategic demands bias the dynamic interactions between these nodes that make up a larger network that support spatial working memory. Here, we used coherence to test this idea and did indeed see changes in the functional interactions with the FEF as a function of the strategic task demands. A network of oculomotor areas was found to be highly interactive during the Match trials. We propose that this network supports working memory by representing and maintaining saccade goals. Another network composed primarily of higher-order prefrontal areas was found to be highly interactive during the Non-Match trials. We propose that this network supports working memory by sustaining covert attention at a particular location (Corbetta et al., 2002). Therefore, different nodes in a larger overlapping network change their patterns of interaction depending on which strategy is employed during spatial working memory tasks.

Acknowledgments

We thank John Ollinger, Ben Inglis, and Vikas Rao for technical assistance. This work was supported by grants from NIH and the James S. McDonnell Foundation (CEC).

References

Bates, J.F., Goldman-Rakic, P.S., 1993. Prefrontal connections of medial motor areas in the rhesus monkey. J. Comp. Neurol. 336, 211–228.

Biswal, B., Yetkin, F.Z., Haughton, V.M., Hyde, J.S., 1995. Functional connectivity in the motor cortex of resting human brain using echo-planar MRI. Magn. Reson. Med. 34, 537–541.

Boussaoud, D., Wise, S.P., 1993. Primate frontal cortex: neuronal activity following attentional versus intentional cues. Exp. Brain Res. 95, 15–27.

Brillinger, D.R., 2001. Time Series Data Analysis and Theory. SIAM, Philadelphia.

Brown, M.R., DeSouza, J.F., Goltz, H.C., Ford, K., Menon, R.S., Goodale, M.A., Everling, S., 2004. Comparison of memory- and visually guided saccades using event-related FMRI. J. Neurophysiol. 91, 873–889.

Corbetta, M., Kincade, J.M., Shulman, G.L., 2002. Neural systems for visual orienting and their relationships to spatial working memory. J. Cogn. Neurosci. 14, 508–523.

Cordes, D., Haughton, V.M., Arfanakis, K., Wendt, G.J., Turski, P.A., Moritz, C.H., Quigley, M.A., Meyerand, M.E., 2000. Mapping functionally related regions of brain with functional connectivity MR imaging. AJNR Am. J. Neuroradiol. 21, 1636–1644.

Courtney, S.M., Petit, L., Maisog, J.M., Ungerleider, L.G., Haxby, J.V., 1998. An area specialized for spatial working memory in human frontal cortex. Science 279, 1347–1351.

Curtis, C.E., D'Esposito, M., 2003. Persistent activity in the prefrontal cortex during working memory. Trends Cogn. Sci. 7, 415–423.

Curtis, C.E., Rao, V.Y., D'Esposito, M., 2004. Maintenance of spatial and motor codes during oculomotor delayed response tasks. J. Neurosci. 24, 3944–3952.

D'Esposito, M., Postle, B.R., Rypma, B., 2000a. Prefrontal cortical contributions to working memory: evidence from event-related fMRI studies. Exp. Brain Res. 133, 3–11.

D'Esposito, M., Ballard, D., Zarahn, E., Aguirre, G.K., 2000b. The role of prefrontal cortex in sensory memory and motor preparation: an event-related fMRI study. NeuroImage 11, 400–408.

Friston, K.J., 1997. Another neural code? NeuroImage 5, 213–220.

Friston, K.J., Frith, C.D., Liddle, P.F., Frackowiak, R.S., 1993. Functional connectivity: the principal-component analysis of large (PET) data sets. J. Cereb. Blood Flow Metab. 13, 5–14.

Funahashi, S., Bruce, C.J., Goldman-Rakic, P.S., 1989. Mnemonic coding of visual space in the monkey's dorsolateral prefrontal cortex. J. Neurophysiol. 61, 331–349.

Funahashi, S., Chafee, M.V., Goldman-Rakic, P.S., 1993. Prefrontal neuronal activity in rhesus monkeys performing a delayed anti-saccade task. Nature 365, 753–756.

Fuster, J.M., Alexander, G.E., 1971. Neuron activity related to short-term memory. Science 173, 652–654.

Gerstein, G.L., Perkel, D.H., 1969. Simultaneously recorded trains of action potentials: analysis and functional interpretation. Science 164, 828–830.

Gnadt, J.W., Andersen, R.A., 1988. Memory related motor planning activity in posterior parietal cortex of macaque. Exp. Brain Res. 70, 216–220.

Grosbras, M.H., Leonards, U., Lobel, E., Poline, J.B., LeBihan, D., Berthoz, A., 2001. Human cortical networks for new and familiar sequences of saccades. Cereb. Cortex 11, 936–945.

Handwerker, D.A., Ollinger, J.M., D'Esposito, M., 2004. Variation of BOLD hemodynamic responses across subjects and brain regions and their effects on statistical analyses. NeuroImage 21, 1639–1651.

Huerta, M.F., Kaas, J.H., 1990. Supplementary eye field as defined by intracortical microstimulation-connections in macaques. J. Comp. Neurol. 293, 299–330.

Huerta, M.F., Krubitzer, L.A., Kaas, J.H., 1987. Frontal eye field as defined by intracortical microstimulation in squirrel-monkeys, owl monkeys, and macaque monkeys: 2. Cortical connections. J. Comp. Neurol. 265, 332–361.

Kubota, K., Niki, H., 1971. Prefrontal cortical unit activity and delayed alternation performance in monkeys. J. Neurophysiol. 34, 337–347.

LaBar, K.S., Gitelman, D.R., Parrish, T.B., Mesulam, M., 1999. Neuroanatomic overlap of working memory and spatial attention networks: a functional MRI comparison within subjects. NeuroImage 10, 695–704.

Leung, H.C., Gore, J.C., Goldman-Rakic, P.S., 2002. Sustained mnemonic response in the human middle frontal gyrus during on-line storage of spatial memoranda. J. Cogn. Neurosci. 14, 659–671.

Lu, M.T., Preston, J.B., Strick, P.L., 1994. Interconnections between the prefrontal cortex and the premotor areas in the frontal lobe. J. Comp. Neurol. 341, 375–392.

Luppino, G., Matelli, M., Camarda, R., Rizzolatti, G., 1993. Corticocortical connections of area F3 (SMA-proper) and area F6 (pre-SMA) in the macaque monkey. J. Comp. Neurol. 338, 114–140.

Miezin, F.M., Maccotta, L., Ollinger, J.M., Petersen, S.E., Buckner, R.L., 2000. Characterizing the hemodynamic response: effects of presentation rate, sampling procedure, and the possibility of ordering brain activity based on relative timing. NeuroImage 11, 735–759.

Miller, L.M., Escabi, M.A., Schreiner, C.E., 2001. Feature selectivity and interneuronal cooperation in the thalamocortical system. J. Neurosci. 21, 8136–8144.

Miller, L.M., Schreiner, C.E., 2000. Stimulus-based state control in the thalamocortical system. J. Neurosci. 20, 7011–7016.

Muller, K., Lohmann, G., Bosch, V., von Cramon, D.Y., 2001. On multivariate spectral analysis of fMRI time series. NeuroImage 14, 347–356.

Muller, K., Mildner, T., Lohmann, G., Von Cramon, D.Y., 2003. Investigating the stimulus-dependent temporal dynamics of the BOLD signal using spectral methods. J. Magn. Reson. Imaging 17, 375–382.

Postle, B.R., Berger, J.S., Taich, A.M., D'Esposito, M., 2000. Activity in human frontal cortex associated with spatial working memory and saccadic behavior. J. Cogn. Neurosci. 12, 2–14.

Quintana, J., Fuster, J.M., 1999. From perception to action: temporal integrative functions of prefrontal and parietal neurons. Cereb. Cortex 9, 213–221.

Rainer, G., Rao, S.C., Miller, E.K., 1999. Prospective coding for objects in primate prefrontal cortex. J. Neurosci. 19, 5493–5505.

Rosenberg, J.R., Amjad, A.M., Breeze, P., Brillinger, D.R., Halliday, D.M., 1989. The Fourier approach to the identification of functional coupling between neuronal spike trains. Prog. Biophys. Mol. Biol. 53, 1–31.

Rowe, J.B., Toni, I., Josephs, O., Frackowiak, R.S., Passingham, R.E., 2000. The prefrontal cortex: response selection or maintenance within working memory? Science 288, 1656–1660.

Sakai, K., Rowe, J.B., Passingham, R.E., 2002. Active maintenance in prefrontal area 46 creates distractor-resistant memory. Nat. Neurosci. 5, 479–484.

Sereno, M.I., Pitzalis, S., Martinez, A., 2001. Mapping of contralateral space in retinotopic coordinates by a parietal cortical area in humans. Science 294, 1350–1354.

Shaw, J.C., 1984. Correlation and coherence analysis of the EEG: a selective tutorial review. Int. J. Psychophysiol. 1, 255–266.

Simon, S.R., Meunier, M., Piettre, L., Berardi, A.M., Segebarth, C.M., Boussaoud, D., 2002. Spatial attention and memory versus motor preparation: premotor cortex involvement as revealed by fMRI. J. Neurophysiol. 88, 2047–2057.

Smith, E.E., Jonides, J., 1999. Storage and executive processes in the frontal lobes. Science 283, 1657–1661.

Stanton, G.B., Bruce, C.J., Goldberg, M.E., 1995. Topography of projections to posterior cortical areas from the macaque frontal eye fields. J. Comp. Neurol. 353, 291–305.

Sun, F.T., Miller, L.M., D'Esposito, M., 2004. Measuring interregional functional connectivity using coherence and partial coherence analyses of fMRI data. NeuroImage 21, 647–658.

Sweeney, J.A., Mintun, M.A., Kwee, S., Wiseman, M.B., Brown, D.L., Rosenberg, D.R., Carl, J.R., 1996. Positron emission tomography study of voluntary saccadic eye movements and spatial working memory. J. Neurophysiol. 75, 454–468.

Zarahn, E., Aguirre, G.K., D'Esposito, M., 1999. Temporal isolation of the neural correlates of spatial mnemonic processing with fMRI. Brain Res. Cogn. Brain Res. 7, 255–268.